Science of the Total Environment 407 (2009) 4838–4851

Contents lists available at ScienceDirect

Science of the Total Environment

journal homepage: www.elsevier.com/locate/scitotenv

Cellular pathology and histopathology of hypo-salinity exposure on the coral *Stylophora pistillata*

Craig A. Downs [a,b], Esti Kramarsky-Winter [c], Cheryl M. Woodley [d], Aaron Downs [e], Gidon Winters [f], Yossi Loya [c], Gary K. Ostrander [a,*]

[a] *Pacific Biosciences Research Center, University of Hawaii at Manoa, 2500 Campus Rd., Hawaii Hall 211, Honolulu, HI 96822, USA*
[b] *Haereticus Environmental Laboratory, P.O. Box 92, Clifford, VA 24533, USA*
[c] *Department of Zoology, George S. Wise Faculty of Life Sciences, Tel Aviv University, Tel Aviv, 69978, Israel*
[d] *US National Oceanic and Atmospheric Administration, CCEHBR, Hollings Marine Laboratory, 331 Ft. Johnson Rd., Charleston, SC 29412, USA*
[e] *Department of Molecular, Cellular and Developmental Biology, Yale University, 266 Whitney Ave., New Haven, CT 06511, USA*
[f] *Department of Plant Sciences, George S. Wise Faculty of Life Sciences, Tel Aviv University, Tel Aviv, 69978, Israel*

ARTICLE INFO

Article history:
Received 1 January 2009
Received in revised form 25 April 2009
Accepted 1 May 2009
Available online 9 June 2009

Keywords:
Cellular diagnostics
Coral
Hypo-salinity
Oxidative stress

ABSTRACT

Coral reefs can experience extreme salinity changes, particularly hypo-salinity, as a result of storms, heavy rainy seasons (e.g., monsoons), and coastal runoff. Field and laboratory observations have documented that corals exposed to hypo-saline conditions can undergo extensive bleaching and mortality. There is controversy in the literature as to whether hypo-saline conditions induce a pathological response in corals, and if there is a relationship between decreasing salinity treatment and pathological responses. To test the hypothesis that hypo-salinity exposure does not have a pathological effect on coral, we used histological and cellular diagnostic methods to characterize the pathology in hypo-salinity-exposed corals. Colonies of *Stylophora pistillata* were exposed to five salinity concentrations [39 parts per thousand (ppt), 32 ppt, 28 ppt, 24 ppt, and 20 ppt] that may realistically occur on a reef. Histological examination indicated an increasing severity of pathomorphologies associated with decreasing salinity, including increased tissue swelling, degradation and loss of zooxanthellae, and tissue necrosis. Pulse-amplitude modulated chlorophyll fluorimetry kinetics demonstrated a decreasing photosynthetic efficiency with decreasing salinity conditions. Cytochrome *P450* levels were affected by even slight changes in salinity concentration suggesting that detoxification pathways, as well as several endocrine pathways, may be adversely affected. Finally, these studies demonstrated that hypo-saline conditions can induce an oxidative-stress response in both the host and in its algal symbiont, and in so doing, may synergistically increase oxidative-stress burdens. As with other types of environmental stresses, exposure to hypo-saline conditions may have long-term consequences on coral physiology.

1. Introduction

Coral reefs can experience extreme changes in salinity of varying duration. Storms, heavy rainy seasons (e.g., monsoons), hurricanes, and coastal runoff can significantly alter surface and depth salinity (Coles and Jokiel, 1992; Devlin et al., 1998; Orr and Moorehouse, 1933; Porter et al., 1999). Over the short term, haloclines of less than 14 ppt can form over in-shore reefs that are quickly dispelled within a few days after heavy rains (Devlin et al., 1998). Long-term exposure to hypo-saline conditions on coral reefs is not uncommon. For example, decreased salinity levels (28–32 ppt) existed for almost a month on coral reefs located centrally on the Great Barrier Reef after heavy storms (Devlin et al., 1998). Studies dating back to 1933, indicate that hypo-salinity is a significant environmental factor that may impact a coral reef and influence the distribution of cnidarian species and populations (Berkelmans and Oliver, 1999; Cloud, 1952; Goreau, 1964; Orr and Moorehouse, 1933). Bleaching and mortality of near-shore corals and anemones are often reported in association with hypo-saline conditions resulting from heavy rainfall events (Berkelmans and Oliver, 1999; Cloud, 1952; Goreau, 1964; Egana and DiSalvo, 1982; Hendy et al., 2003; Lirman et al., 2008; Orr and Moorehouse, 1933; Van Woesik et al., 1995). In the laboratory, hypo-salinity induced bleaching in corals and anemones is an established phenomenon characterized by pathologies, including reduced photosynthetic efficiency and altered metabolism of respiratory pathways (Engebretson and Martin, 1994; Hoegh-Guldberg and Smith, 1989; Moberg et al., 1997; Tytlianov et al., 2000). These metabolic pathologies can in turn influence higher-order physiological diseases, such as gamete abnormalities and reduced viabilities, significantly affecting fecundity (Richmond, 1993).

* Corresponding author. 2500 Campus Way, 211 Hawaii Hall, Honolulu, HI 96821, USA. Tel.: +1 808 956 7837; fax: +1 808 956 2751.
E-mail address: gko@hawaii.edu (G.K. Ostrander).

0048-9697/$ – see front matter © 2009 Elsevier B.V. All rights reserved.
doi:10.1016/j.scitotenv.2009.05.015

Corals are osmo-conformers, becoming iso-osmotic with their surroundings, gaining water when exposed to hypo-saline conditions (Rankin and Davenport, 1981; Tytlianov et al., 2000). Hypotonic conditions can cause damage within a number of different organelles and cellular fractions (Jahnke and White, 2003; Maeda and Thompson, 1986). Mitochondria, in particular, are among of the most vulnerable cell structures to osmotic damage; changes in osmolarity can disrupt mitochondrial electron transport and alter NADH redox capacity, producing an increase in reactive oxygen species and altering cellular metabolism (Ballantyne and Moon, 1986; Martinez et al., 1995; Shivakumar and Jayaraman, 1986). Mitochondrial enzymes that play key roles in amino acid metabolism in invertebrates are depressed in response to hypo-saline conditions (Devin et al., 1997; Ellis et al., 1985; Moyes et al., 1986). Osmotic shifts induce adverse changes in endoplasmic reticulum structure and lysosomal function in plant and animal cells (Nicholson, 2001). In the chloroplast, hypotonicity can inhibit photosynthetic electron transport and catalase activity (Allen 1977; Asada 1999; Burdon et al., 1996; Lockau, 1979). Hypo-tonicity has been shown to block induction of the heat-shock protein response in hepatocytes, thus reducing their ability to deal with stress (Kurz et al., 1998). In contrast to higher invertebrate and vertebrate pathologies associated with hypo-saline conditions, there have been few studies that examine the physiological responses of coral to this environmental condition. The majority of these studies have focused on the effects of hypo-salinity on photosynthesis of the coral's zooxanthellae, or general respiration of coral symbiosis (Alutoin et al., 2001; Kershwell and Jones 2004; Manzello and Lirman, 2003).

To test the hypothesis that increasing hypo-salinities result in an increase in histopathological and cellular pathological phenomena, *Stylophora pistillata* were exposed to five salinity regimes (39 parts per thousand (ppt), 32 ppt, 28 ppt, 24 ppt, and 20 ppt). Changes in cellular structure/function and mechanisms of stress induced by hypo-saline conditions were examined by measuring cellular processes (protein chaperoning and degradation, xenobiotic response, oxidative stress and response, Photosystem II efficiency) in control and hypo-saline exposed corals, as well as associated microscopic structural changes.

2. Methods

2.1. Materials

All chemicals for buffered solutions were obtained from Sigma-Aldrich (St Louis, MO). Histological reagents were obtained from Electron Microscopic Sciences (Hatfield, PA). Polyvinylidene fluoride (PVDF) membrane was obtained from Millipore Corp. (Bedford, MA). Antibodies against all the cellular parameters, as well as calibrant standards, were gifts from EnVirtue Biotechnologies, Inc. (Winchester, VA). Anti-rabbit conjugated horseradish peroxidase antibodies were obtained from Jackson ImmunoResearch Laboratories, Inc. (West Grove, PA). DNA extraction kits and DNA purification and DNA AP site assay kits were obtained from Dojindo Molecular Technologies (Gaithersburg, MD).

2.2. Collection and growth condition of S. pistillata

Ten fragments, 2–3 cm in length, were collected from each of eight *S. pistillata* colonies from the reef near the H. Steinitz Marine Biological Laboratory in Eilat, Israel. The fragments were transported to the lab in seawater-filled plastic bags. Each fragment was tied at its base using monofilament fishing line and hung from a rubber hose in outdoor flow-through sea water aquaria maintained at ambient sea temperatures (24 °C). The aquaria were shaded by neutral density shade cloth that allowed 50% ambient irradiance. The fragments were allowed to acclimate for a period of two months prior to experimentation. Only fragments exhibiting healing at fragmentation lesions, growth, characteristic color, and free of gross lesions were deemed healthy and used for exposure experiments.

2.3. Stress exposures

S. pistillata fragments were exposed to varying salinities of sea water made by diluting the ambient sea water (39 ppt) with distilled water that had the same pH as the sea water. Colony genotypes were randomly distributed among the five treatments and aquaria-treatments were randomly distributed. All tanks were static flow and aerated. The five experimental exposures were 39 ppt, 32 ppt, 28 ppt, 24 ppt and 20 ppt. A fragment from each colony was hung in each treatment aquarium (total of 8 fragments per treatment). Exposures were carried out for 24 h, followed by photographic documentation of each fragment and measurement of chlorophyll fluorescence parameters. The samples were then immediately frozen in liquid nitrogen and stored at −80 °C until analysis.

2.4. Sample preparation, Enzyme-Linked Immunosorbent Assay (ELISA) validation, and ELISA

Coral samples were ground to a fine powder using liquid nitrogen-chilled ceramic mortars and pestles. Samples (~10 mg) of frozen tissue were placed in 1.8 ml microcentrifuge tubes containing 1600 µl of a denaturing buffer consisting of 2% sodium dodecyl sulfate (SDS), 50 mM Tris–HCl (pH 7.8), 25 mM dithiothreitol, 10 mM disodium ethylenediaminetetraacetic acid (EDTA), 0.001 mM sorbitol, 3% polyvinylpolypyrrolidone (wt/vol), 0.001 mM alpha-tocopherol, 0.005 mM salicylic acid, 0.01 mM 4-(2-Aminoethyl) benzenesulfonyl fluoride hydrochloride (AEBSF), 0.04 mM Bestatin, 0.001 mM E-64, 2 mM phenylmethylsulfonyl fluoride (PMSF), 0.5 mM benzamidine, 5 µM α-amino-caproic acid, and 1 µg/100 µl pepstatin A. Samples were heated at 92 °C for 3 min, vortexed for 20 s, incubated at 92 °C for another 3 min, and then incubated at 25 °C for 5 min. Samples were centrifuged at 10,000 ×*g* for 5 min. Supernatant free of a lipid/glycoprotein mucilage matrix was transferred to a new tube, and protein concentration was determined by the method of Ghosh et al., 1988.

Antibodies used in this study were raised against an 8–12 residue polypeptide conjugated to ova albumin and immuno-purified with a Pierce SulfoLink Kit (Thermo Scientific, Rockford, IL, cat.# 44895) using the original unconjugated peptide as the affinity binding agent. Antigens were designed based on highly conserved and unique domains found within the target protein. The antigen sequences were generated by comparing cDNA-translated protein sequences from cnidarians, other invertebrate taxa (e.g., *C. elegans*, *Drosophila*, etc), and plant/algae using alignment analysis in the ClustalW software from the Accelyrs Gene software service pack. A domain was identified as unique to one taxa (invertebrate vs plant), and confirmed using BLAST analysis that it was not shared by any other class of protein in Genbank and Swiss Protein Bank, as well as our own in-house gene banks for cnidarians (Downs et al., 2009, private and public — www.marinegenomics.org).

One-dimensional SDS-polyacrylamide gel electrophoresis (SDS-PAGE) and western blotting were used to validate each antibody used in ELISA assays involving *S. pistillata*. One-hundred and twenty micrograms of total soluble protein from three randomly prepared samples were pooled and 10 µg of total soluble protein per lane was loaded onto either a 12.5% or 15% SDS-PAGE analytical gel (8 cm). A Tris(2-carboxyethyl)phosphine hydrochloride (TCEP; neutral pH) concentration of 0.001 M was added to the separating portion of the gel. All gels were blotted unto PVDF membranes using a wet-transfer electro-blotting system. The membrane was blocked in 7% non-fat dry milk, and assayed with the primary antibody for 1 h at room temperature. The blots were washed in Tris-buffered saline pH 7.8 (TBS)

four times each for 15 min, and incubated in a horseradish peroxidase-conjugated secondary antibody solution for 1 h at room temperature. Blots were washed four times as above in TBS, and developed using a NEN Western Lightning Plus (Perkin-Elmer, Waltham, MA) luminol/hydrogen peroxide-based chemiluminescent solution and documented using a Syngene (Frederick, MD) Genegnome luminescent documentation system.

Once validated, antibodies and samples were optimized for ELISA format using an $8\times6\times4$ factorial design (Crowther, 2001). Samples were subject to ELISA assay using a Beckman–Coulter Biomek 2000 with 384-well microplates. Samples were assayed using the following antibodies and EnVirtue catalog numbers: algal anti-glutathione peroxidase (GPx) (AB-G101-P), algal anti-heat-shock protein 60 (AB-H100-P), algal anti-heat-shock protein 70 (AB-H101-P), algal anti-chloroplast small heat-shock protein (AB-CHsHSP), anti-ubiquitin (AB-U100), cnidarian anti-heat-shock protein 70 (AB-H101-CDN), invertebrate Grp75 (AB-GRP75I), invertebrate anti-heat-shock protein 60 (AB-H100-IN), invertebrate polymerized/single anti-ubiquitin (AB-UBI), invertebrate ubiquitin activase E1 (AB-ULE1), invertebrate anti-manganese superoxide dismutase (MnSOD) AB-S100-MM), cnidarian glutathione-s-transferase (GST) (pi-isoform homologue; AB-GST-INV), invertebrate anti-small heat-shock protein (AB-H103), invertebrate ferrochelatase (AB-FC), invertebrate Heme Oxygenase Type 1 (AB-HO1IN), invertebrate protoporphyrinogen oxidase IX (Ab-PPO-IN), invertebrate catalase (AB-CAT3), invertebrate cytochrome *P450* 2 (AB-CY2), invertebrate cytochrome *P450* 3 (Ab-CY3), cnidarians Cu/Zn superoxide dismutase (Ab-CZSOD), algal Cu/Zn superoxide dismutase (Ab-A-CZSOD), animal MutY DNA Glycosylase (Ab-MtY), invertebrate cytochrome *P450* 6 (AB-CY6), DNPH (protein carbonyl), and anti-MXR (multi-xenobiotic resistance protein, ABC family of proteins; P-glycoprotein 180; AB-MDR-180). Samples were assayed in triplicate with intra-specific variation of less than 12% for the whole plate. An eight-point calibrant curve using a calibrant relevant to each antibody was plated in triplicate for each plate.

DNA was isolated according to manufacturer's instructions using the Dojindo Get pureDNA kit-Cell, tissue (catalog # GK03-20). DNA concentrations were determined using an Invitrogen/Molecular Probes Quant-iT™ DNA Assay Kit, Broad Range (catalog # Q33130, Carlsbad, CA) using either a Shimadzu spectrofluorophotometer or a Bio-Tek fluorescent microplate reader with the appropriate excitation/emission filters. DNA AP concentration was determined using the Dojindo DNA Damage Quantification Kit-AP Site Counting (DK-02-10) and was conducted according to manufacturer's instructions with one exception. Instead of using a colorimetric reporter system as the manufacturer recommended, we used NEN Western Lightning Plus luminol/hydrogen peroxide-based chemiluminescent solution as part of the detection system since the horseradish peroxide conjugate in the kit can also use luminol as a substrate. Light detection was measured using a Bio-Tek 800 fluorescent/luminescent microplate reader.

2.5. Pulse-amplitude modulated (PAM) chlorophyll fluorimetry

Optimal quantum yield of Photosystem II (F_v/F_m; see Björkman and Demmig-Adams, 1987) was measured using a PAM chlorophyll fluorometer (Diving-PAM; Walz, Germany; Schreiber et al., 1997). The F_v/F_m ratio indicates the physiological well being of the electron transfer chain within the photosystem. Following a 24-hour exposure to each salinity regime, measurements were performed on 4–7 fragments within each treatment after dark-adapting all corals for 1 h, using the leaf distance clip to allow the same angle and distance for all coral pieces.

2.6. Histology

Fragments from each exposure were fixed in 4% formalin in seawater (at the appropriate osmolarity) for 24 h then rinsed in filtered seawater and maintained in 70% ethanol/30% seawater. The fragments were decalcified using a 1:1 (v/v) solution of 50% formic acid and 20% sodium citrate. The tissue was then processed in an automated Shandon Citadel tissue processor embedded in paraffin and sectioned (5 μm). At least five slides per treatment from at least three individuals per treatment were made. Each slide mount came from a different area and depth in the tissue. Comparisons were made between slides from the same area (in terms of tissue depth, or polyp area) for each treatment. Each slide had five to six 5 μm-thick serial sections. The sections were stained with hematoxylin /eosin and observed and photographed.

2.7. Statistical analysis

Data were tested for normality using the Kolmogorov–Smirnov test (with Lilliefors' correction) and for equal variance using the Levene Median test. If the data were normally distributed and homogeneous, a one-way analysis of variance (ANOVA) was employed. When data did not meet the homogeneity of variances requirement for one-way ANOVA, we used Kruskal–Wallis One-Way Analysis of Variance on Ranks. When significant differences were found among treatment means, we used the Tukey–Kramer Honestly Significant Difference (HSD) method or the Holm–Sidak test as an exact alpha-level test to determine differences among each of the treatments (Sokal and Rohlf, 1995).

We used canonical correlation analysis (CCA) as a heuristic tool to illustrate how biomarkers could be used to discriminate between populations. Canonical correlation analysis is an eigen-analysis method that reveals the basic relationships between two matrices (Gauch, 1985), in our case those of the five treatments and biomarker data. The CCA provided an objective statistical tool for (1) determining if populations are different from one another using sets of cellular biomarkers that are indicative of a cellular process (e.g., protein chaperoning and degradation, xenobiotic response), and (2) which biomarkers contributed to those differences. This analysis required combining data from all five treatments into one matrix, which we did by expressing biomarker responses in a given treatment as a proportion of their mean levels.

3. Results

3.1. Antibody validation

Antibodies against cnidarian and dinoflagellate cellular parameters did not exhibit significant non-specific cross-reactivity (Fig. 1), hence could be validly used in an ELISA format. All blots presented in these figures were exposed for long periods of time (1 min, 38 s); a technique to reveal subtle non-specific cross-reactivities that may confound ELISA measurements. ELISA-microplate readings are based on a four-second exposure. The levels of sensitivity between the Syngene Genegnome documentation system and the Bio-Tek fluorescent/luminescence microplate reader are approximately equal, hence, the non-specific, faint bands are non-detectable by the microplate reader. Because of the evolutionary conservation of ubiquitin these antibodies detected proteins from the host and symbiotic zooxanthellae in the coral homogenate (data not shown), consequently an ELISA measurement using this antibody can detect total protein concentration.

The western blot for dinoflagellate Hsp70 showed two expected bands between ~70 and 75 kilo units (ku; Standard international; Fig 1C) (Rensing et al., 1994). Antibody to metallothionein type-1 exhibited two bands around 5–6 ku; invertebrates often have several alleles and isoforms of type 1, and cnidarians have at least two homologs (Fig 1F) (Brouwer et al., 1992; Snell et al., 2003). Ferrochelatase is a ~40–48 ku protein and is often expressed as two isoforms in invertebrates as well as in *Nematostella* (Fig 1G) (Dailey, 1990; Putnam et al., 2007; Shibahara et al., 2007). Heme Oxygenase I

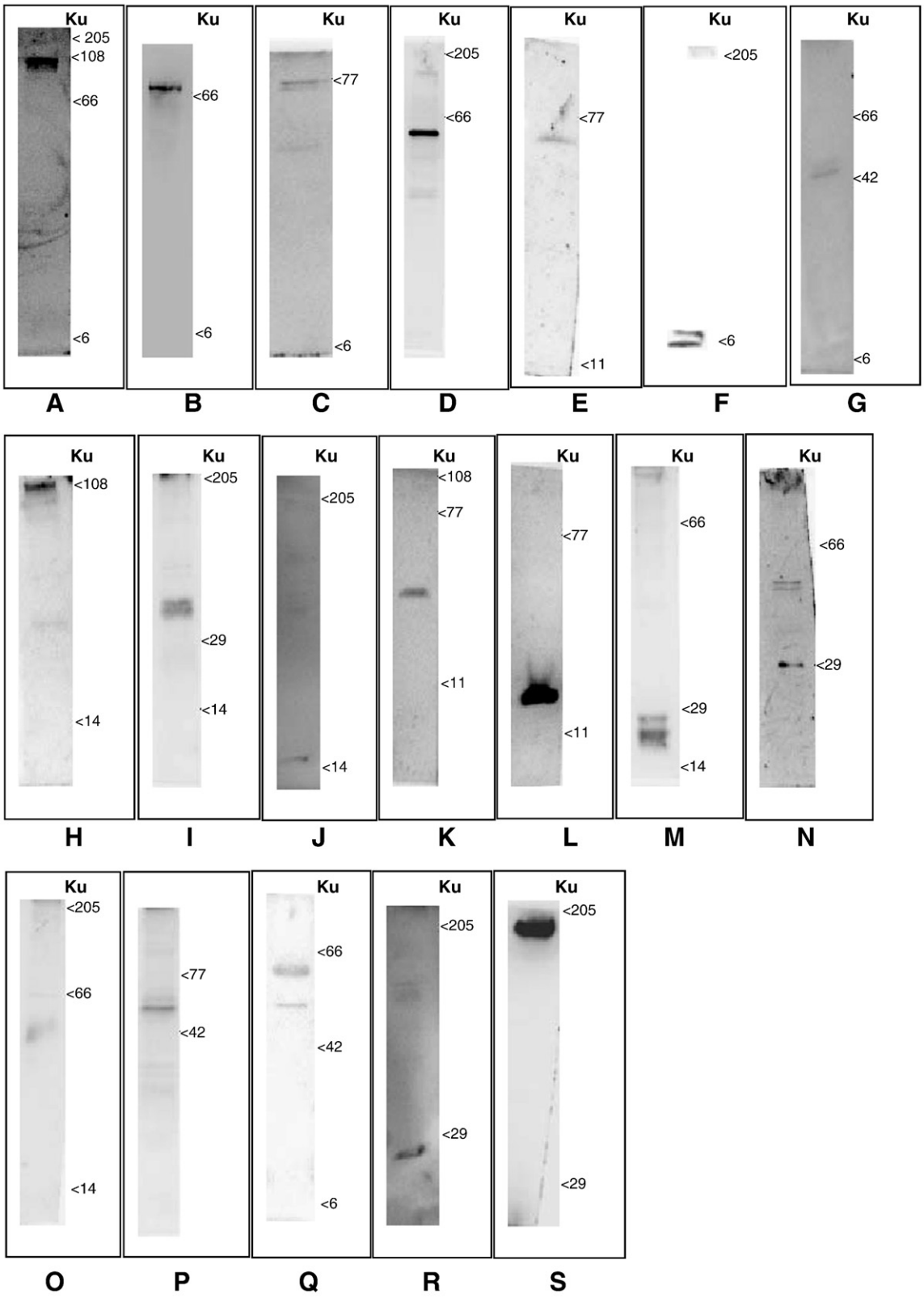

Fig. 1. Western blots as validation for ELISA. Corals were homogenized and subjected to SDS-PAGE (5 μg total soluble protein per lane), western blotting, and assayed with polyclonal antibody specific for the target protein. The migration rate for each band is indicated with the following blots: A = Hsp90 (85–98 ku); B = Hsp70 cnidarian (70–75 ku); C = Hsp70 dinoflagellate (70–78 ku); D = Hsp60 cnidarian (58–65 ku); E = Hsp60 dinoflagellate (60–65 ku); F = metallothionein I cnidarians (~5 ku); G = ferrochelatase cnidarians (40 ku); H = aconitase cnidarians (108 ku); I = Heme Oxygenase I cnidarians (35 ku); J = Cu/ZnSOD cnidarians (20 ku); K = Cu/ZnSOD dinoflagellate (38 ku); L = MnSOD cnidarians (24 ku); M = GPx cnidarians (19 ku); N = GPx dinoflagellate (29 ku and 45–50 ku); O = catalase cnidarians (50–55 ku); P = cytochrome *P450* 2 cnidarian (50–55 ku); Q = cytochrome *P450* 6 cnidarian (50 and 58 ku); R = GST cnidarians (25 ku); S = MDR, both cnidarian and dinoflagellate isoforms (160 and 180 ku).

presented as a doublet, which is consistent with a known number of Heme Oxygenase I gene sequences in a related cnidarian species, *Nematostella* (Fig. 1I) (Putnam et al., 2007). Antibody to the cnidarian glutathione peroxidase was raised against the conserved domain containing the selenocystene reactive site, which is found in a number of glutathione peroxidase isoforms, as indicated in the triple banding pattern in Fig. 1M (Brigelius-Floh, 1999; Putnam et al., 2007). Two classes of plant/algal cytosolic glutathione peroxidases (GPx1 and 2) are apparent in Fig. 1N, exhibiting two isoforms ~45 ku (GPx2) and the GPx1 isoform at 29 ku. These two isoforms share a highly conserved ligand-binding domain that was used to design the target antigen for this antibody based on known sequences in *Nematostella* and *Acropora palamta* (Putnam et al., 2007; Rodriguez et al., 2003). The western blot for catalase showed a single band ~55 ku (Fig 1O), the smudge is from non-specific cross-reactivity as a result of uneven blocking. Antibody against a conserved domain unique to members of the cytochrome *P450* 2-family detected three species of CYP 2 ~50 to 55 ku (Fig. 1P), similar to the expression of CYP 2 species found in the coral, *Porites lobata* (Downs et al., 2006; Goldstone, 2008; Reitzel et al., 2008). The western blot for the cytochrome *P450* 6-family (Fig. 1Q) presented two distinct bands; one band ~53 ku and a slow-migrating band ~58 ku (Bhaskara et al., 2006; Reitzel et al., 2008).

3.2. ELISA results

ELISA for dinoflagellate Hsp60, dinoflagellate Hsp70, cnidarian Grp75, cnidarian Hsp60, cnidarian Hsp70, cnidarian ubiquitin activase, total ubiquitin, chloroplast sHsp and the four major cnidarian sHsp classes were performed to address the possibility of differences in *Protein chaperoning and degradation* between the hypo-salinity treatments (Table 1). Cnidarian Hsp70 and Grp75, which are two Hsp70 homologues, and ubiquitin significantly increased in response to salinity levels 28 ppt and lower. Ubiquitin activase and cnidarian Hsp60 were more sensitive to changes in salinity, and significantly increased at 32 ppt salinity and lower. Cnidarian small Hsps were the least sensitive to changes in salinity, and were only detectable at salinities of 24 ppt and lower. Dinoflagellate Hsp60 and the chloroplast sHsp only changed their expressions at 28 ppt and lower. Canonical correlation analysis indicates distinct changes in protein chaperoning and degradation when exposed to a regime of decreasing salinities (Fig. 2A; Wilks' Lambda value = 0.0041032; F Test < 0.0001).

ELISA for dinoflagellate Cu/ZnSOD, dinoflagellate GPx, cnidarian MnSOD, cnidarian Cu/ZnSOD, cnidarian catalase, invertebrate MutY, DNA AP lesion, and protein carbonyl were performed to access potential differences in *oxidative-stress response* among treatments (Table 1). Cnidarian anti-oxidant defenses were very responsive to the small changes in salinity, and their induction preceded detectable changes in protein oxidation. In contrast, the DNA repair enzyme, MutY, only accumulated at the lowest salinity concentration. Dinoflagellate anti-oxidant enzymes responded in a similar fashion as the cnidarian anti-oxidant enzymes, except that at 20 ppt, dinoflagellate Cu/ZnSOD protein levels either decreased to a point where the protein levels were below the calibrant standard curve or the epitope that is recognized by the antibody had been masked (e.g., adduction with an aldehyde such as 4-hydroxynonenal or oxidized). DNA damage as reflected by the accumulation of DNA abasic lesions (apurinic/apyrimidinic site) on DNA more than tripled when corals were exposed to 28 ppt salinity, and increased by almost seven fold when exposed to 20 ppt salinity (Table 1). Canonical correlation analysis showed a significant shift in anti-oxidant defenses and an accumulation of biochemical lesions associated with oxidative damage from exposure to a decreasing salinity regime, and that the 24–20 ppt treatment was defined predominantly

Table 1
Unless otherwise noted all data are presented as fmol/ng total soluble protein (TSP).

Cellular parameter	39 ppt	32 ppt	28 ppt	24 ppt	20 ppt
Protein chaperoning and degradation					
Hsp70 cnidarian	195 ± 21^{a}	207 ± 13^{a}	170 ± 26^{a}	330 ± 34^{b}	424 ± 31^{b}
Grp75 cnidarian	108 ± 2^{a}	70 ± 4^{b}	96 ± 7^{a}	45 ± 7.4^{c}	33 ± 3^{c}
Hsp60 cnidarian	5 ± 0.3^{a}	$8 \pm 0.5^{a,b}$	$11 \pm 1^{b,c}$	9 ± 0.6^{c}	12 ± 0.3^{d}
Ubiquitin	120 ± 9^{a}	157 ± 15^{a}	158 ± 7^{a}	$169 \pm 13^{a,b}$	218 ± 12^{b}
Ubiquitin activase E1 cnidarian	589 ± 16^{a}	750 ± 21^{b}	801 ± 38^{b}	894 ± 29^{c}	1110 ± 76^{d}
Small heat-shock proteins cnidarian	2.8 ± 0.4^{a}	4.3 ± 0.2^{b}	7.7 ± 1.7^{a}b	27.7 ± 4.1^{c}	33.6 ± 2.7^{c}
Hsp60 dinoflagellate	70 ± 11^{a}	114 ± 14^{a}	228 ± 19^{b}	523 ± 46^{c}	595 ± 31^{c}
Chloroplast small heat-shock protein	5 ± 1^{a}	6 ± 12^{a}	16 ± 5^{a}	72 ± 23^{b}	132 ± 40^{b}
Oxidative damage and response					
Protein carbonyl	3 ± 0.6^{a}	10 ± 3^{a}	32 ± 9^{b}	332 ± 41^{c}	526 ± 43^{d}
Catalase cnidarian	17 ± 5^{a}	$28 \pm 8^{a,b}$	$45 \pm 3^{b,c}$	$42 \pm 5^{b,c}$	63 ± 6^{c}
Cu/ZnSOD cnidarian	53 ± 5^{a}	70 ± 3^{a}	$77 \pm 6^{a,b}$	$111 \pm 7^{b,c}$	185 ± 16^{c}
MnSOD cnidarian	259 ± 7^{a}	447 ± 8^{b}	383 ± 18^{c}	672 ± 57^{d}	1179 ± 24^{e}
MutY cnidarian	81 ± 10^{a}	$95 \pm 5^{a,b}$	77 ± 12^{a}	89 ± 3^{a}	128 ± 7^{b}
Cu/ZnSOD dinoflagellate	140 ± 11^{a}	215 ± 34^{b}	447 ± 25^{c}	712 ± 31^{d}	BCC^{e}
GPx-1 dinoflagellate	99 ± 13^{a}	101 ± 12^{a}	203 ± 39^{b}	341 ± 11^{c}	424 ± 28^{d}
Porphyrin metabolism					
PPO cnidarian	2.7 ± 0.2^{a}	2.9 ± 0.09^{a}	2.6 ± 0.05^{a}	2.7 ± 0.02^{a}	2.6 ± 0.08^{a}
Ferrochelatase cnidarian	14 ± 2^{a}	12 ± 0.2^{a}	13 ± 1^{a}	11 ± 0.6^{a}	18 ± 1^{a}
Heme Oxygenase 1 cnidarian	22 ± 2^{a}	31 ± 2^{a}	30 ± 3^{a}	$34 \pm 3^{a,b}$	46 ± 5^{b}
DNA damage					
DNA AP site (per 1×10^{5} nucleotides)	137 ± 19^{a}	124 ± 25^{a}	428 ± 42^{b}	540 ± 34^{b}	947 ± 58^{c}
Xenobiotic response					
CYP P450 2 cnidarian	4.8 ± 0.3^{a}	4.4 ± 0.5^{a}	2.4 ± 0.3^{b}	1.3 ± 0.1^{c}	1.5 ± 0.2^{c}
CYP P450 3 cnidarian	6 ± 0.5^{a}	12 ± 0.5^{b}	12 ± 1.3^{b}	12 ± 0.8^{b}	15 ± 2^{b}
CYP P450 6 cnidarian	29 ± 2^{a}	7 ± 0.4^{b}	7 ± 0.5^{b}	11.2 ± 0.3^{b}	9 ± 0.7^{b}
GST-pi cnidarian	103 ± 13^{a}	86 ± 7^{a}	126 ± 40^{a}	120 ± 7^{a}	142 ± 19^{a}
MXR	1.1 ± 0.2^{a}	1.0 ± 0.05^{a}	1.2 ± 0.3^{a}	1.3 ± 0.07^{a}	1.1 ± 0.2^{a}

Entries in the table give treatment means ± 1 SE. If the data were normally distributed and homogeneous, a one-way analysis of variance (ANOVA) was employed. When data did not meet the homogeneity of variances requirement for one-way ANOVA, we used Kruskal–Wallis One-Way Analysis of Variance on Ranks. Treatment means with different superscripted letters differed significantly at $\alpha = 0.05$ using the Tukey–Kramer HSD method, Holm–Sidak test, Student–Newman–Keuls Method or Dunn's Test. BCC = below calibrant curve.

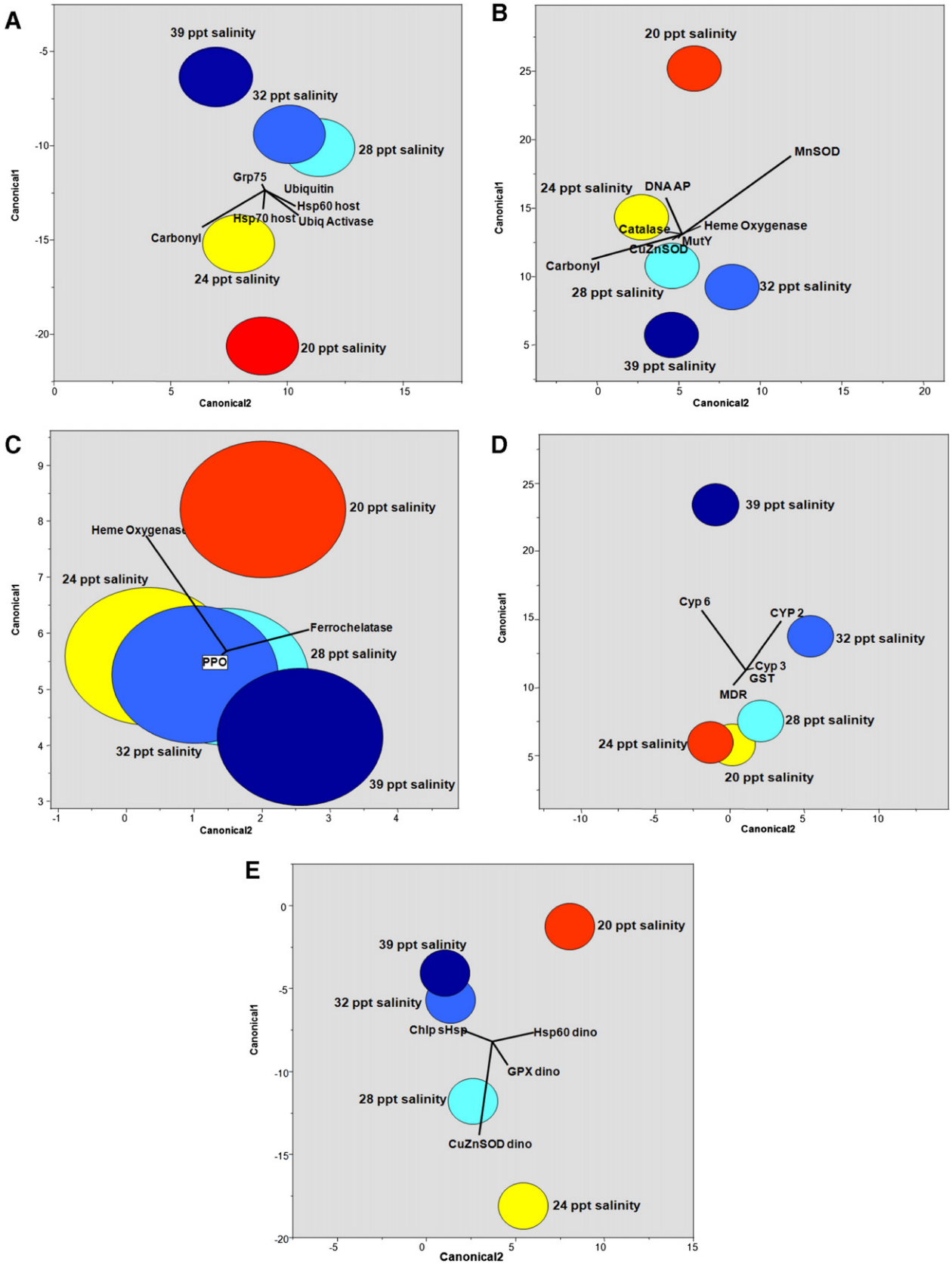

Fig. 2. Canonical centroid plot of biomarkers. Canonical correlation analysis was used to address the question: are the biomarker patterns of a particular metabolic category affected by the five salinity treatments. Original variates were biomarker levels expressed as a percentage of the control value in each treatment. Circles show the 95% confidence intervals around the distribution centroid of each stressor. Biplot rays radiating from the grand mean show directions of original biomarker responses in canonical space. Overlapping centroids indicate that those salinity treatments are not significantly different from one another, while non-overlapping centroids indicate a difference. (A) Protein metabolism biomarkers: non-overlapping centroids have an *R* value of less than 0.16. (B) Oxidative-stress biomarkers: non-overlapping centroids have an *R* value of less than 0.09. (C) Porphyrin metabolism biomarkers: non-overlapping centroids have an *R* value of less than 0.11. (D) Xenobiotic-response biomarkers: non-overlapping centroids have an *R* value of less than 0.04. (E) Dinoflagellate stress markers: non-overlapping centroids have an *R* value of less than 0.02.

by accumulation of these cellular lesions (Fig. 2B; Wilks' Lambda value = 0.0001228, *F* Test < 0.0001).

ELISA for cnidarian ferrochelatase, protoporphyrinogen oxidase IX (PPO) and Heme Oxygenase 1 (HO1) were performed to assay differences in *porphyrin metabolism* between the salinity treatments. Ferrochelatase and PPO levels showed no changes in response to salinity. In contrast, HO1 levels were significantly elevated at 20 ppt salinity and lower (Table 1). Canonical correlation analysis showed no significant difference between 39 ppt and salinities of 32 ppt and 28 ppt, though there was a significant difference between 39 ppt and 24 and 20 ppt salinities (Fig. 2C; Wilks' Lambda value = 0.1090869, *F* Test < 0.0001).

ELISA for cnidarian GST-pi, cnidarian cytochrome *P450* 6, and MXR was performed to investigate differences in *xenobiotic response* between treatments (Table 1). Neither GST nor MXR showed a response to any salinity treatment. Cytochrome *P450* 3-family showed a significant increase in response to hypo-salinity (Table 1). Cytochrome *P450* 2-family exhibited a significant decrease to hypo-saline treatments of 28 ppt and lower. Cytochrome *P450* 6-family showed a marked decrease in expression level in response to all hypo-saline treatments. Canonical correlation analysis indicated a marked change in cellular condition related to xenobiotic response capacity (Fig. 2D; Wilks' Lambda value = 0.0029262, *F* Test < 0.0001).

3.3. PAM chlorophyll fluorescence

Decreases in seawater salinity were found to correlate strongly ($r = 0.9$, $P < 0.05$) with decreases in the optimal quantum yield of PSII (F_v/F_m; Fig. 3). While exposure of corals to 39–32 ppt resulted in normal F_v/F_m values for the season in which we performed this experiment, exposing coral fragments to 28 ppt and lower resulted in a significant (one-way ANOVA, $P < 0.05$) decrease in F_v/F_m values (Fig. 3).

3.4. Histology

Overall, changes in polyp integrity were visible at all hypo-saline concentrations. The extent of change observed in gross tissue architecture of the coral fragments increased as the exposure salinity decreased (Figs. 4–6). At 32 ppt and below, coral tissues swelled and lost their coloration, with the change most pronounced at 28 ppt. Microscopic examination showed disruption of tissue architecture, necrosis, and pyknosis. At 28 ppt, tissue confluence disruption was clearly evident, particularly in the gastrodermal tissue layer.

Control corals exhibited well defined tissue layers with a columnar cell epidermal layer. The nuclei were elongate and positioned in the basal two-thirds of the cells in this tissue layer. Mucus cells and nematocytes, particularly spirocysts, were abundant (Fig. 4A, E). In these fragments, the gastrodermis was replete with zooxanthellae. Corals from the 32 ppt treatment (Fig. 4B) showed a breakdown in the columnar characteristics of the epidermal layer in the oral disc region. There was a decrease in the number of mucus cells and a possible breakdown of nematocytes. The most prominent difference between control and 32 ppt exposed corals was the presence of eosinophilic extra-cytoplasmic inclusion bodies. These were apparent in the gastrodermal layer as opposed to the epithelia. Co-occurring with hyper-eosinophilia, gastrodermal cells also suffered from the loss of normal cellular architecture and zooxanthellae, vacuolization, and the presence of non-staining bodies (Fig. 4B, black arrow pointing left). At 28 ppt, the epidermis retained its integrity but this tissue was best characterized by pyknosis of the nuclei, loss of mucus cells and nematocytes, and the occurrence of eosinophilic extra-cytoplasmic inclusion bodies (Fig. 4C, D). The stomadeal epidermis showed increased pyknosis at 28 ppt, as compared to 32 ppt, and further loss of cellular architecture. Gastrodermal tissue disruption was also exacerbated, as characterized by cell debris in both tissue layers, a loss of most zooxanthellae, with those remaining swollen in appearance (Fig. 4F).

Gonads were evident in all fragments at all salinities (Figs. 5 and 6). Planulae from fragments maintained at lower salinities showed increases in the breakdown of tissue and increased nuclear pyknosis (Fig. 5C–F). In fragments from hypo-saline treatments, oocytes appeared normal though the tissue was swollen and cell confluence was disrupted surrounding the oocytes (Fig. 6B). Although gross testes architecture was maintained, microscopic changes in tissue architecture were evident. Spermatids within the testes were swollen at the lower salinity (Fig. 6F).

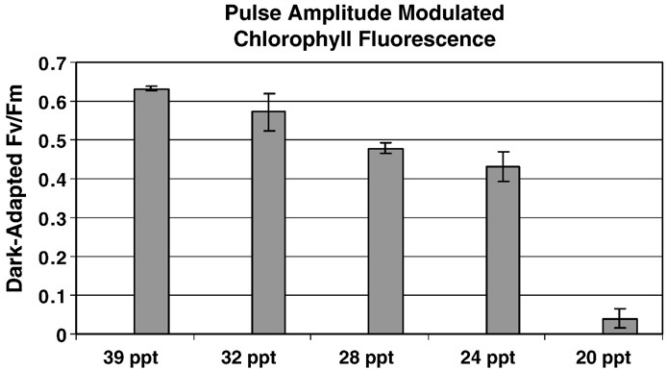

Fig. 3. Dark-adapted F_v/F_m in *Stylophora pistillata* measured using a DIVING-PAM chlorophyll fluorometer. All measurements were performed using the leaf distance clip, following 24 h of exposure to the different salinities, and after dark-adapting all coral fragments for 1 h. $n = 4$–7 replicates per treatment, +/− SE.

4. Discussion

Among the primary causes of coral reef decline identified by the Pew Oceans Commission and the US Commission on Ocean policy are a reduction in water quality resulting from runoff and pollution from land-based and marine sources (Pew Ocean Commission, 2003). Though its presence is readily observable (e.g., haloclines) and measurable, hypo-salinity is often disregarded as a significant factor in coral reef decline, because it is difficult to link it to changes occurring in the landscape of adjoining watersheds (i.e., a single point source) (Fabricius, 2005).

We have demonstrated that *S. pistillata* responds to hypo-saline conditions at gross, cellular, and biochemical of levels. Gross morphological changes to hypo-salinity showed (1) increased tissue swelling, degradation, and loss of zooxanthellae with decreasing salinities, (2) paling (bleaching) of the brownish-yellow coloration of the tissue associated with maintenance of a healthy population of zooxanthellae, (3) an increase in pink fluorescent coloration at the lowest salinity (20 ppt), and (4) tissue necrosis at the two lowest salinity concentrations (20 and 24 ppt).

Histologically, changes were observed in the cellular integrity and tissue architecture with these changes occurring to differing degrees in different tissues. Changes in the symbiont's photosynthetic capacities and pathways were detected using PAM chlorophyll fluorimetry kinetics.

One of the most important findings of this study is that hypo-salinity induces an oxidative-stress response in both the host and the symbiont, and that there is a linear relationship between decreasing saline conditions and increasing burdens of oxidative stress.

4.1. Protein chaperoning and degradation

Protein chaperoning and degradation is the cellular status of protein synthesis, protein maturation, and protein degradation. Changes

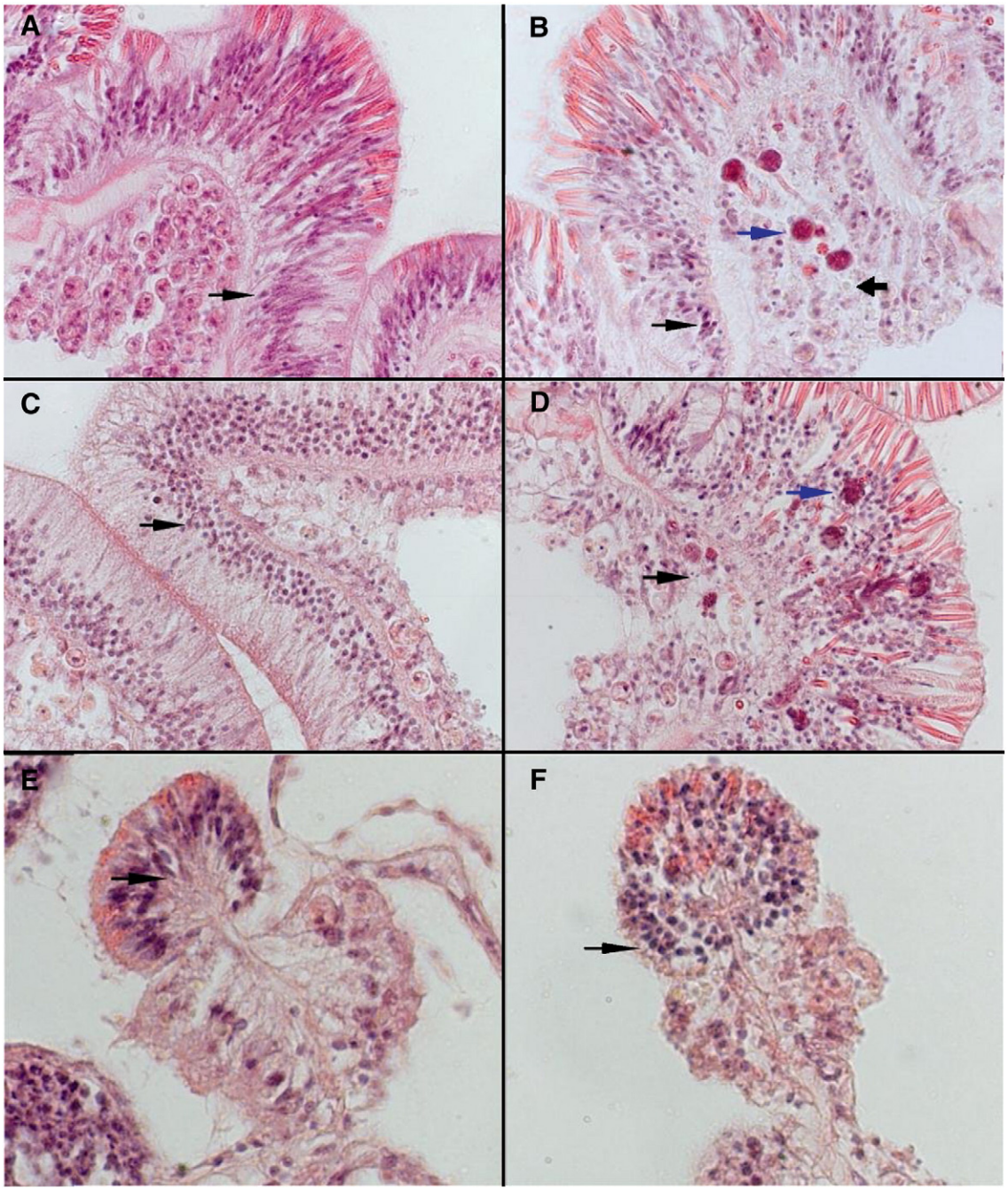

Fig. 4. *Stylophora pistillata* polyp tissue. (A) Ambient salinity (39 ppt): section of stomadeal area (×20). Arrows denote nuclei. (B) 32 ppt section of stomadeal area. Blue arrow denotes cell necrosis in the epidermis black arrows point to cells undergoing disintegration as denoted by hyper-eosinophylia (×20). (C) 28 ppt. Arrow denotes the rounded nuclei cellular degradation is evident by increased vacuolization. (D) 28 ppt section of stomadeal area. Gastrodermal cells loss of architecture. Black arrow denotes pyknosis. (×20) (E) Septal filament from control coral. Note the abundance of mucus cells and columnar integrity of the epithelium. (F) Septal filaments of coral from 28 ppt: note loss of cellular integrity and the rounding of the nuclei.

in any of these processes are indicative of a significant change in cellular metabolism and homeostasis (Downs, 2005). In this study, only six parameters of protein chaperoning and degradation in cnidarians and two parameters in the dinoflagellate were examined, but whose changes in behavior are indicative of a wider system response. Thus, these biomarkers were used to test the hypothesis that hypo-saline conditions significantly shifted the concentration of these parameters. Heat-shock protein 70 (Hsp70) is a cytosolic chaperonin, while Grp75 is the mitochondrial homologue. The cytosolic Hsp70 function is a crucial element in the maturation of newly made proteins to gain their active state. GRP75 is essential in the maturation of newly imported proteins into the mitochondria. The ability to reassemble denatured proteins is often the most commonly recognized function of both Hsp70 and Grp75 (Ellis, 1996; Papp et al., 2003). Cnidarian heat-shock protein 60 (Hsp60) is the major mitochondrial chaperonin and functions to mature nuclear-encoded, mitochondrial-imported proteins into their active state (Ellis, 1996). Elevation of this protein signifies that there has been a general shift in the protein chaperoning and degradation within the mitochondria and implies a change in the equilibria of mitochondrial-associated metabolic pathways (Papp et al., 2003). The dinoflagellate Hsp60 homologue is better known as the RuBisCO-binding protein and was first discovered to chaperone RuBisCO, the primary enzyme of the Calvin Cycle in photosynthesis (Hemmingsen, 1990; Jackson-Constan et al., 2001). Ubiquitin could be

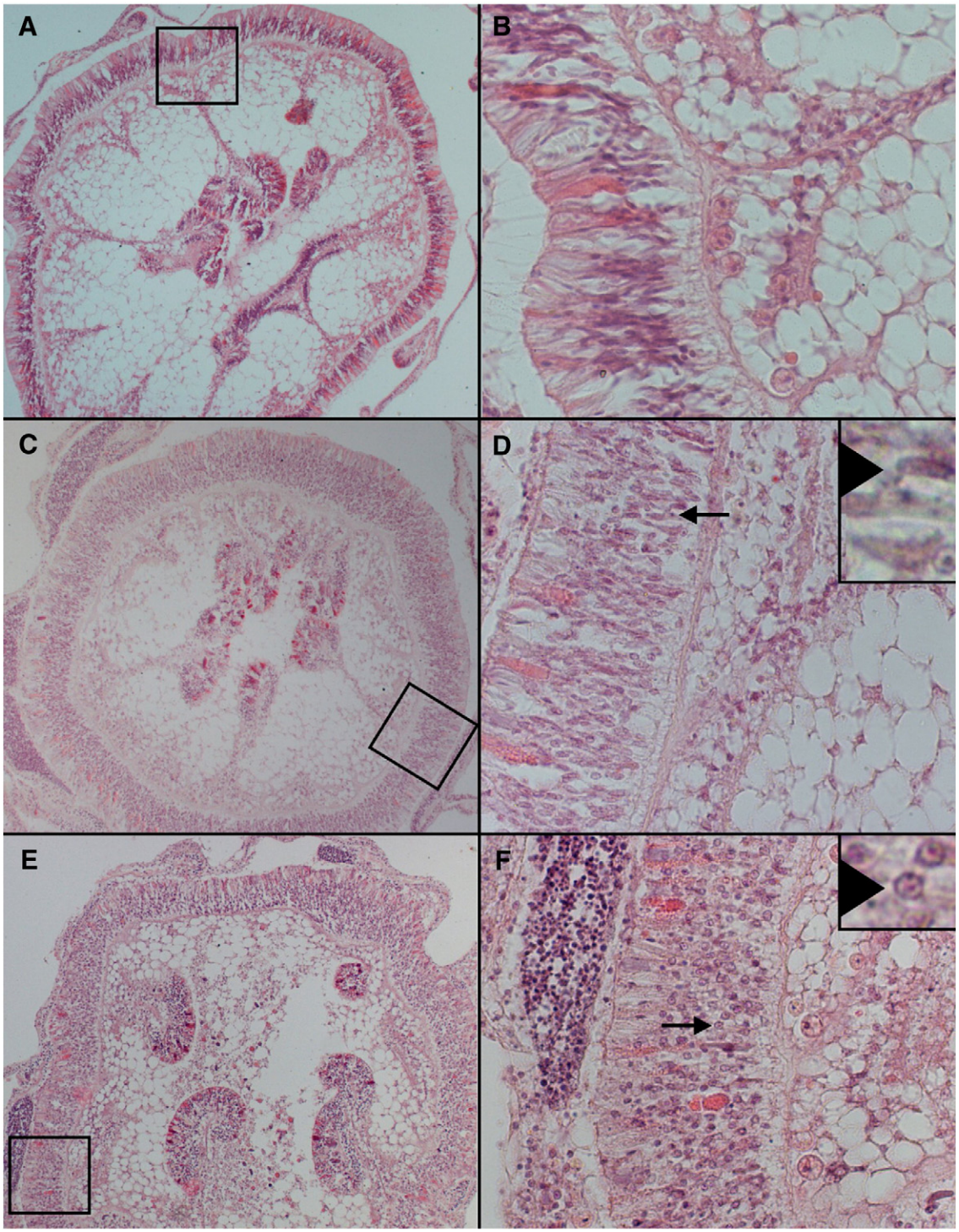

Fig. 5. *Stylophora pistillata* planulae. Histological sections from fragments maintained at different salinities: (A) Ambient (control) salinity (×10). (B) Close-up of boxed area (×40) showing cell structure; note the well defined columnar nature of epidermal layer of the planulae, intact zooxanthellae. (C) Planula from coral in 32 ppt (×10). (D) Close-up of boxed area showing cell structure (×40). Arrows indicate nuclei, note the breakdown of tissue. (E) Planulae from coral in 28 ppt (×10) (F) Close-up of boxed area (×40) showing cell structure. Arrows indicate nuclear pyknosis as well as loss of cellular integrity.

considered the 'death mark' of proteins; its conjugation to broken or no-longer-needed proteins marks these proteins for degradation (Hershko and Ciechanover, 1998). Ubiquitin activase E1 prepares and mediates the conjugation catalysis event between ubiquitin and the target protein and an increase in activity suggests amplification of protein degradation processes (Shang et al., 1997).

The cnidarian and chloroplast small heat-shock proteins (sHsps) are often absent under normal conditions, but are induced only as a result of severe stress (Downs et al., 1999). Measurement of cnidarian sHsps in this study was actually the measurement of five separate isozymes (sHsps 16, sHsp22, sHsp23, sHsp26, sHsp28), because the antibody used in the study binds to a highly conserved epitope that is found only on these five proteins. Each of these sHsps is independently regulated and localizes to different places within the cell, and perhaps to different tissue types (Branton et al., 1999; De Jong et al., 1993; Heckathorn et al., 1999; Morrow et al., 2004; Willsie and Clegg, 2002). The chloroplast sHsp specifically associates with the oxygen evolving complex of Photosystem II and protects Photosystem II

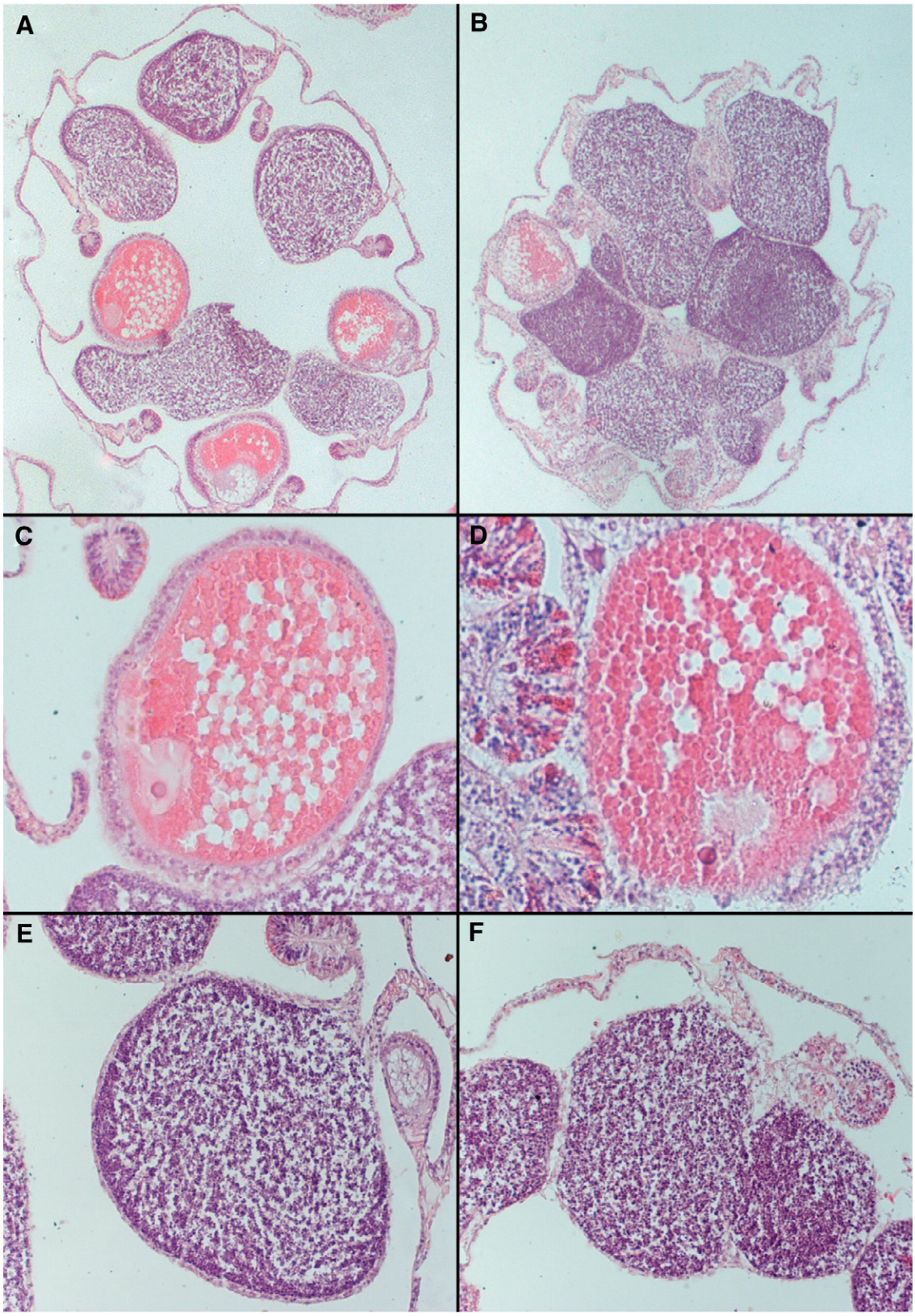

Fig. 6. *Stylophora pistillata* gonad tissue. Histological sections from fragments maintained at different salinities: (A) Polyp from ambient (control) salinity, 39 ppt, ×10. (B) Hypo-saline treatment, 28 ppt, ×10. (C) Oocyte from control coral (note defined nucleus and nucleolus). (D) Oocyte from 28 ppt fragment. Note loss of architecture of the follicular tissue surrounding the oocyte. (E) Testes from control (39 ppt) coral. (F) Testes from 28 ppt treatment. Note swelling of the gonad and the loss of architecture of the tissue surrounding the testes.

activity during heat stress, ultraviolet-radiation exposure, and oxidative stress, most likely via a recycling anti-oxidant mechanism (Downs et al., 1999; Heckathorn et al., 1999).

Canonical correlation analysis indicates distinct changes in protein chaperoning and degradation when corals are exposed to a regime of decreasing salinities (Fig. 2A). The first proteins to respond

to the change in salinity were Hsp60 and ubiquitin activase. Lack of induction of Hsp70, ubiquitin, and the sHsps at 32 ppt suggests that the organism was responding to a stressor, but was not responding to a cellular crisis (a condition defined by the presence of cellular lesions) (Halliwell and Gutteridge, 1999). For example, neither protein carbonyl, nor DNA damage, was evident at this salinity. This is supported by histological evidence that showed only slight changes in cellular architecture at this salinity. On the other hand, all the host biomarkers for protein chaperoning and degradation at 28 ppt were significantly elevated in comparison to controls, indicating a marked shift in cellular condition. This condition is marked by an accumulation of cellular lesions, specifically oxidized proteins and damage to DNA, likely the result of nucleotide oxidation. The effects of this treatment were morphologically evident in the widespread changes to coral tissue and cellular architecture. Specific changes were evidenced by the nuclear rounding and cell degradation. At 24 ppt, there is an increase in tissue degradation with a significant accumulation of the sHsps, indicating a serious alteration of metabolic structures and processes (Ornatsky et al., 1995). Grp75 levels were reduced at 24 ppt and 20 ppt, which may have been a result of the mitochondrial-import rate being adversely affected by oxidative and osmotic stress (Papp and Nardai, 2003; Takahashi and Hood, 1996). For the dinoflagellate, Hsp60 chaperonin did not significantly accumulate until exposure to 28 ppt salinity. Together, these individual responses form a diagnostic profile showing that decreasing salinity regimes will shift protein chaperoning and degradation from a situation characterized by a coordinated increase in the rate of protein synthesis and protein degradation to a metabolic condition with a significant increase in the rate of protein degradation relative to protein synthesis (Ellis, 1996; Downs, 2005; Hershko and Ciechanover, 1998).

4.2. Oxidative-stress response

A cell is able to withstand the adverse effects of oxidative stress based on its ability to (1) suppress reactive oxygen species generation (2) neutralize reactive oxygen species once they are formed, and (3) repair the damage to a cellular structure caused by lesions generated from reactive oxygen species (Halliwell and Gutteridge, 1999). Canonical correlation analysis showed a significant shift in anti-oxidant defenses and an accumulation of cellular lesions associated with oxidative damage from exposure to a decreasing salinity regime (Fig. 2B). The enzymes that respond to the 32 ppt salinity exposure were catalase, dinoflagellate Cu/ZnSOD, and MnSOD, indicating that hypo-salinity induced an oxidative-stress response, but no major change in tissue morphologies was visible. Protein oxidation was not apparent until exposure to 28 ppt salinity when tissue breakdown was widespread and cellular debris was prevalent in both the epidermis and gastrodermal tissues (Fig. 4). Induction of MutY was not apparent until 20 ppt salinity, even though DNA AP lesions significantly accumulated at higher salinities. One explanation for this result is that MutY repair activity can increase without an increase in accumulation of the enzyme. Thus the concentration of MutY at 28 and 24 ppt salinity may have been sufficient to repair oxidized base pairs. The accumulation of DNA lesions at 20 ppt may have been so severe that it overwhelmed the basal capacity of MutY to repair the DNA lesions.

Dinoflagellate anti-oxidant enzymes exhibited a similar pattern to host anti-oxidant enzyme profiles, indicating that the dinoflagellate was also responding to an oxidative-stress insult (Fig. 2E). Severe photo-oxidative stress can cause inactivation and degradation of Cu/ZnSOD, as well as masking of epitopes by making the domain unrecognizable as a result of oxidative cleavage (non-protease dependent) and aldehyde adduction (Casano et al., 1997; Kurepa et al., 1997; Sakaguchi et al., 2004).

4.3. Porphyrin metabolism

Porphyrins are essential ligands used by proteins in a number of physiological processes, such as oxidative phosphorylation, steroidogenesis and fatty acid synthesis, and xenobiotic responses (Ajioka et al., 2006). Shifts in the porphyrin metabolic equilibrium reflect a major shift in cellular metabolism as a whole (Marks et al., 1982; Thunell and Harper 2000). Protoporphryinogen oxidase IX catalyzes the penultimate step of porphyrin production and ferrochelatase the last step, inserts iron into the porphyrin ring to form hemin (Dailey, 1990; Dailey et al., 2000). Heme Oxygenase I catalyzes the decomposition of heme to biliverdin, carbon monoxide, and ferrous iron (Schwartsburd, 2001). Biliverdin is further catalyzed to bilirubin, which is a powerful lipophilic anti-oxidant (Stocker and Ames, 1987). Interestingly, the porphyrin synthesis pathway was unaltered by hypo-salinity exposure as indicated by a lack of change in both ferrochelatase and protoporphryinogen oxidase IX (Fig. 2C; Table 1). The porphyrin degradation pathway however was altered when corals were exposed to salinities of 24 ppt and lower, though most likely not in response to damaged porphyrins, but rather from a need to increase bilirubin's anti-oxidant potential (Stocker and Ames, 1987).

4.4. Xenobiotic response

Cells can regulate and expel potentially harmful xenobiotics through a three-phase process. In Phase I, xenobiotics undergo an enzymatically catalyzed reaction that introduces a polar group into the xenobiotic's molecular composition that can impart toxicity, or confer an enhanced toxicity compared to the parent compound (Jokanović, 2001). Enzymes responsible for such reactions include the superfamily of cytochrome *P450*s, the flavin-containing monooxygenases, and a host of esterases (Ronis et al., 1996). In Phase II, these new polar metabolites are conjugated with endogenous substrates such as sulfates, acetates, glutathione, and glucuronides (Jokanović, 2001; Glatt et al., 2001; Negishi et al., 2001; Ronis et al., 1996). These new hydro-soluble products can now be managed by the cell for transport to lysosomes for further metabolism, sequestered into lysosome-like structures for containment, or excreted from the cell through active diffusion transporters, such as the ATP-binding cassette transporters (Borst and Elferink, 2002).

Canonical correlation analysis indicated a marked change in cellular condition related to xenobiotic response capacity (Fig. 2D). Cytochrome *P450* 3 exhibited a slight tendency to increase at higher salinity treatments. This is in stark contrast to the sharp decrease in levels of both cytochrome *P450* 2 and 6 in response to hypo-saline treatments. Cytochrome *P450* 6 is an invertebrate subfamily of P450s that is known to oxidize and be up-regulated by pesticides such as aldrin, dieldrin, diazinon, chlorpyrifos, deltamethrin, and a wide range of pyrethroid compounds (Dunkov et al., 1997; Scott and Wen, 2001). In mammals and some invertebrates, cytochrome *P450* 2 monooxygenase can be induced by ethanol, carbon tetrachloride, and PCBs congeners. This protein class also plays a significant role in steriodogenesis (Lieber, 1997; Ronis et al., 1996). Decrease of this protein class by hypo-salinity may affect not only the coral's ability to defend against xenobiotics, but it may affect steroidogenesis, which in turn can affect reproductive processes.

4.5. PAM chlorophyll fluorescence

The ratio of F_v/F_m is an index that reflects the efficiency of open Photosystem II reaction centers. While the maximal F_v/F_m values for a wide variety of terrestrial plants range between 0.830 and 0.833 (Björkman and Demmig-Adams, 1987), the values for zooxanthellae within healthy-looking corals (measured with a Diving-PAM) range between 0.565 and 0.65 (depending on season and depth).

Several studies have demonstrated the severe reduction in F_v/F_m values measured for *in hospite* zooxanthellae exposed to severe stress and have correlated this with expulsion of zooxanthellae, i.e., coral bleaching (Bhagooli and Hidaka, 2003; Jones and Hoegh-Guldberg, 1999). During the 1998 bleaching event in the Florida Keys, F_v/F_m values of bleached corals ranged between 0.35 and 0.47 (Warner et al., 1999). Although a relatively short-duration stress experiment, PAM measurements in our experiment indicate that zooxanthellae exposed to anything less than 28 ppt suffered severe damage to their algal photosynthetic apparatus, leading to impairment of photosynthesis. This is in agreement with a recent study by Kershwell and Jones (2004) who showed that a significant decrease of F_v/F_m values occurred only at salinities of 26 ppt or lower (10 ppt lower than ambient).

4.6. Histology

Gross observations indicated no apparent distress of corals exposed to 32 ppt salinity. However, histological examination showed obvious tissue and cellular damage, which was only exacerbated with decreasing salinities. Comparison of histological plates in Fig. 4 shows a change in the staining of the mesoglea, both in the central matrix and along the basal layer of the mesoglea; eosin staining becomes less pronounced in the hypo-saline samples. Cnidaria have the most primitive nervous system with primary axons potentially extending beyond the mesoglea, but with the neural cell found largely along the basal boundaries of the mesoglea (Grimmelikhuijzen et al., 1996). Eosin-staining cells, with hematoxylin stained nuclei that run along the mesoglea boundaries, can be seen in the control plate (Fig. 4A), but this structure becomes more difficult to recognize in samples from hypo-saline exposures.

The effect on gonadal tissue is striking (Fig. 6). Oocytes exhibited significant changes in internal architecture, including what appears to be rupturing of the nuclear membrane and displacement of the nucleolus. Follicular cells within the gonadal repository showed extensive disorganization and a reduction in eosin staining. Disruption of the gonadal tissue strongly suggests that exposure to hypo-saline conditions may have a detrimental effect on the reproductive fitness of the exposed coral. Basic reproductive studies need to be conducted to confirm this effect.

Although exposure of these fragments to hypo-saline conditions was not prolonged, some cellular damage was visible at all hypo-saline conditions. Most of the effect could be attributed to "osmotic swelling" and it is likely that this resulted in some electrolyte depletion. It is possible that if this effect is relatively short-lived, the coral may recuperate quickly. The histological changes such as the hyper-eosinophilic bodies found in the tissues of colonies from the lower salinities may represent one type of effect that hypo-salinity has on the cellular structure of coral tissues.

4.7. Conclusion

The histological and biomarker evidence provided here indicate it is possible that the effect of a short-lived inundation of these corals by fresh water (that reduces salinity by not more than 9 ppt) is reversible. This inference is also supported by Hoegh-Guldberg and Smith (1989) who showed no effect on oxygen flux and biomass of zooxanthellae in *S. pistillata* from the Great Barrier Reef maintained at a salinity of 5 ppt lower than ambient salinity. They did find, though, that corals exposed to 23 ppt (12 ppt lower than ambient) all died following a 36-hour exposure. The *S. pistillata* colonies in this study showed similar changes; there were no discernible macro-changes in corals exposed to salinities of 7 ppt below ambient (i.e., 32 ppt), however, histological and cellular parameter changes were observed. Exposure of fragments to lower salinities (i.e., below 28 ppt) for 24 h did result in extreme biochemical and histological changes accompanied by extreme degradation and necrosis. This suggests that the possibility of recuperation following such an osmotic shock may be relatively low and that the range of salinities in which these corals may osmo-conform is relatively narrow. Since *S. pistillata* colonies found in the northern Gulf of Aqaba (Eilat) (average yearly rainfall approximately 3 cm/year) are not usually exposed to low salinities, it is not surprising that these corals have minimal tolerance to drastic and prolonged changes in salinity. The histological changes occurring in zooxanthellae and coral cells corroborate the results obtained by the PAM fluorescence and biomarkers of cellular metabolism.

The integration of biochemical, morphological and cellular metabolism features into a diagnostic profile allows for an in-depth understanding of the response coral cells have to be environmental stress and their ability to withstand these stresses. Such knowledge is of particular value in light of the predicted environmental changes from global warming, rising seawater levels and changes occurring in coastal land usage. As a result of coastal development, the mortality and bleaching associated with corals and other coral reef organisms (e.g., sea urchins) is a recent social concern and a significant factor for environmental impact assessment and natural resource damage investigations (Coles and Jokiel, 1992; Devlin et al., 1998; Muthiga and Szmant, 1987; Porter et al., 1999).

Acknowledgements

This work was funded by EnVirtue Biotechnologies, Inc., the Israeli Science Foundation (ISF), Haereticus Environmental Laboratory, and the Raynor Chair for Environmental Conservation Research at Tel Aviv University. We sincerely thank Maytal Balushtein, Nachshon Siboni, and Roee Segal for their generous help in conducting the coral collection, culturing, and exposure for this experiment. We also thank Robert Richmond for editing the manuscript and Ross Jones for discussions concerning coral physiology and hypo-salinity.

This publication does not constitute an endorsement of any commercial product or intend to be an opinion beyond scientific or other results obtained by the U.S National Oceanic and Atmospheric Administration (NOAA). No reference shall be made to NOAA, or this publication furnished by NOAA, to any advertising or sales promotion which would indicate or imply that NOAA recommends or endorses any proprietary product mentioned herein, or which has as its purpose an interest to cause the advertised product to be used or purchased because of this publication.

References

Ajioka RS, Phillips JD, Kushner JP. Biosynthesis of heme in mammals. Biochim Biophys Acta 2006;1763:723–36 2006.
Allen JF. Effects of washing and osmotic shock on catalase activity of intact chloroplast preparations. FEBS Lett 1977;84:221–4.
Alutoin S, Boberg J, Nystroem M, Tedengren M. Effects of the multiple stressors copper and reduced salinity on the metabolism of the hermatypic coral *Porites lutea*. Mar Environ Res 2001;52:289–99.
Asada K. The water–water cycle in chloroplasts: scavenging of active oxygen and dissipation of excess photons. Annu Rev Plant Physiol Plant Mol Biol 1999;50:601–40.
Ballantyne JS, Moon TW. Solute effects on mitochondria from an elasmobranch (*Raja erinacea*) and a teleost (*Pseudopleuronectes americanus*). J Exp Zool 1986;239:319–28.
Berkelmans R, Oliver JK. Large-scale bleaching of corals on the Great Barrier Reef. Coral Reefs 1999;18:55–60.
Bhagooli R, Hidaka M. Comparison of stress susceptibility of in hospite and isolated zooxanthellae among five coral species. J Exp Mar Biol Ecol 2003;291:181–97.
Bhaskara S, Dean ED, Lam V, Ganguly R. Induction of two cytochrome *P450* genes, Cyp6a2 and Cyp6a8 of *Drosophila melanogaster* by caffeine in adult flies and in cell culture. Gene 2006;377:56–64.
Björkman O, Demmig-Adams B. Photon yield of O_2 evolution and chlorophyll characteristics at 77K among vascular plants of diverse origins. Planta 1987;170:489–504.
Borst P, Elferink RO. Mammalian ABC transporters in health and disease. Annu Rev Biochem 2002;71:537–92.
Branton MA, MacRae TH, Lipschultz F, Wells PG. Identification of a small heat shock/a-crystallin protein in the scleractinian coral *Madracis mirabilis* (Duch. and Mitch.). Can J Zool 1999;77:675–82.

Brigelius-Floh ER. Tissue-specific function of individual glutathione peroxidases. Free Radic Biol Med 1999;27:951–65.
Brouwer M, Schlenk D, Ringwood AH, Brouwer-Hoexum TM. Metal-specific induction of metallothionein isoforms in the blue crab, *Callinectes sapidus*, in response to single and mixed-metal exposure. Arch Biochem Biophys 1992;294:461–8.
Burdon RH, O'Kane D, Fadzillah N, Gill V, Boyd PA, Finch RR. Oxidative stress and responses in *Arabidopsis thaliana* and *Oryza sativa* subjected to chilling and salinity stress. Biochem Soc Trans 1996;4:469–72.
Casano LM, Gomez LD, Lascano HR, Gonzalez CA, Trippi VS. Inactivation and degradation of CuZn–SOD by active oxygen species in wheat chloroplasts exposed to photooxidative stress. Plant Cell Physiol 1997;38:433–40.
Coles SL, Jokiel PL. Effects of salinity on coral reefs. In: Connell DW, Hawker DW, editors. Pollution in tropical aquatic systems. Boca Raton, FL: CRC Press; 1992. p. 147–66.
Cloud PE. Preliminary report on geology and marine environments of Onotoa Atoll, Gilbert Islands. Atoll Res Bull 1952;12:1-73.
Crowther JR. The ELISA guidebook. Totowa, New Jersey: Humana Press; 2001.
Dailey HA. Conversion of coproporphyrinogen to protoheme in higher eukaryotes and bacteria. In: Dailey HA, editor. Biosynthesis of heme and chlorophylls. New York: McGraw-Hill; 1990. p. 123–55.
Dailey HA, Dailey TA, Wu CK, Medlock AE, Wang FK, Rose JP, et al. Ferrochelatase at the millennium: structures, mechanisms, and [2Fe–2S] clusters. CMLS Cell Mol Life Sci 2000;57:1909–26 2000.
De Jong WW, Leunissen JA, Voorter CE. Evolution of the alpha-crystallin/small heat-shock protein family. Mol Biol Evol 1993;10:103–26.
Devin A, Guerin B, Rigoulet M. Control of oxidative phosphorylation in rat liver mitochondria: effect of ionic media. Biochim Biophys Acta 1997;1319:293–300.
Devlin M, Taylor J, Brodie J. Flood plumes, extent, concentration and composition. GBRMPA Reef Res 1998;8:1–9.
Downs CA. Cellular Diagnostics and its application to aquatic and marine toxicology. In: Ostrander G, editor. Techniques in aquatic toxicology, vol. 2. CRC Press, Inc.; 2005. p. 181–207.
Downs CA, Ryan SL, Heckathorn SA. The chloroplast small heat-shock protein: evidence for a general role in protecting photosystem II against oxidative stress and photoinhibition. J Plant Physiol 1999;155:488–96.
Downs CA, Richmond RH, Mendiola WH, Rougée L, Ostrander GK. Cellular-physiological effects of the MV Kyowa Violet fuel oil-spill incident on the coral, *Porites lobata*. Environ Toxicol Chem 2006;25:3171–80.
Downs CA, Kramarsky-Winter E, Martinez J, Kushmaro A, Woodley CM, Loya Y, et al. Symbiophagy and coral bleaching. Autophagy 2009;5:1–6.
Dunkov BC, Guzov VM, Mocelin G, Shotkoski F, Brun A, Amichot M, et al. The *Drosophila* cytochrome P450 gene CYP6a2: structure, localization, heterologous expression, and induction by phenobarbitol. DNA Cell Biol 1997;16:1345–56.
Egana AC, DiSalvo LH. Mass expulsion of zooxanthellae by Easter Island corals. Pac Sci 1982;36:61–3.
Ellis RJ. Stress proteins as molecular chaperones. In: Van Eden W, Young DB, editors. Stress proteins in medicine. New York: Marcel Dekker Inc; 1996.
Ellis LL, Burcham JM, Paynter KT, Bishop SH. Amino acid metabolism in euryhaline bivalves: regulation of glycine accumulation in ribbed mussel gills. J Exp Zool 1985;233:347–58.
Engebretson H, Martin KLM. Effects of decreased salinity on expulsion of zooxanthellae in the symbiotic sea anemone *Anthopleura elegantissima*. Pac Sci 1994;48:446–57.
Fabricius KE. Effects of terrestrial runoff on the ecology of corals and coral reefs: review and synthesis. Mar Pollut Bull 2005;50:125–46.
Gauch HGJ. Multivariate analysis in community ecology. New York: Cambridge University Press; 1985.
Ghosh S, Gepstein S, Heikkila JJ, Dumbroff BG. Use of a scanning densitometer or an ELISA plate reader for measurement of nanogram amounts of protein in crude extracts from biological tissue. Anal Biochem 1988;169:227–33.
Glatt H, Boeing H, Engelke CE, Ma L, Kuhlow A, Pabel U, et al. Human cytosolic sulphotransferases: genetics, characteristics, toxicological aspects. Mutat Res 2001;482: 27–40.
Goldstone JV. Environmental sensing and response genes in cnidaria: the chemical defensome in the sea anemone *Nematostella vectensis*. Cell Biol Toxicol 2008;24:483–502.
Goreau TF. Mass expulsion of zooxanthellae from Jamaican reef communities after hurricane Flora. Science 1964;145:383–6.
Grimmelikhuijzen CJP, Leviev LI, Carstensen K. Peptides in the nervous systems of cnidarians: structure, function, and biosynthesis. Int Rev Cyt 1996;167:37–89 1996.
Halliwell B, Gutteridge JMC. Free radicals in biology and medicine. 3rd ed. Oxford, England: Oxford Science Publications; 1999.
Heckathorn SA, Downs CA, Coleman JS. Small heat-shock proteins protect electron transport in chloroplasts and mitochondria during stress. Am Zool 1999;39:865–76.
Hemmingsen SM. The plastid chaperonin. Semin Cell Biol 1990:47–54.
Hendy EJ, Lough JM, Gagan MK. Historical mortality in massive porites from the central great barrier reef, Australia: evidence for past environmental stress? Coral Reefs 2003;22:207–15.
Hershko A, Ciechanover A. The ubiquitin system. Ann Rev Biochem 1998;67:425–79.
Hoegh-Guldberg O, Smith GJ. The effect of sudden changes in temperature, light and salinity on the population density and export of zooxanthellae from the reef coral *Stylophora pistillata* Esper *and Seriatopora hystrix* Dana. J Exp Mar Biol Ecol 1989;129:279–303.
Jackson-Constan D, Akita M, Keegstra K. Molecular chaperones involved in chloroplast protein import. Biochim Biophys Acta 2001;1541:102–13.
Jahnke LS, White AL. Long-term hypo-saline and hypersaline stresses produce distinct antioxidant responses in the marine algae *Dunaliella tertiolecta*. J Plant Physiol 2003;160:1193–202.
Jokanović M. Biotransformation of organophosphorus compounds. Toxicology 2001;166:139–60.
Jones RJ, Hoegh-Guldberg O. Effects of cyanide on coral photosynthesis: implications for identifying the cause of coral bleaching and for assessing the environmental effects of cyanide fishing. Mar Ecol Prog Ser 1999;177:83–91.
Kershwell AP, Jones R. The effects of hypo-osmosis on the coral *Stylophora pistillata*: the nature and cause of low salinity bleaching. Mar Ecol Prog Ser 2004;253:145–54.
Kurepa J, Herouart D, Van Montagu M, Inze D. Differential expression of CuZn- and Fe-superoxide dismutase genes of tobacco during development, oxidative stress, and hormonal treatments. Plant Cell Physiol 1997;38:463–70.
Kurz AK, Schliess F, Haussinger D. Osmotic regulation of the heat shock response in primary rat hepatocytes. Hepatology 1998;28:774–81.
Lieber CS. Cytochrome P-450 2E1: its physiological and pathological role. Physiol Rev 1997;77:517–44.
Lirman D, Orlando B, Macia S, Manzello D, Kaufman L, Biber P, et al. Coral communities of Biscayne Bay, Florida and adjacent offshore areas: diversity, abundance, distribution, and environmental correlates. Aquat Conserv Mar Freshwat Ecosys 2008;13:121–35.
Lockau W. The inhibition of photosynthetic electron transport in spinach chloroplasts by low osmolarity. Eur J Biochem 1979;94:365–73.
Maeda M, Thompson Jr GA. On the mechanism of rapid plasma membrane and chloroplast envelope expansion in *Dunaliella salina* exposed to hypoosmotic shock. J Cell Biol 1986;102:289–97.
Manzello D, Lirman D. The photosynthetic resilience of *Porites furcata* to salinity disturbance. Coral Reefs 2003;22:537–40.
Marks GS, Zelt DT, Cole SP. Alterations in the heme biosynthesis pathway as an index of exposure to toxins. Can J Physiol Pharmacol 1982;60:1017–26.
Martinez F, Pardo JP, Flores-Herrera O, Espinosa-Garcia MT. The effect of osmolarity on human placental mitochondria function. Int J Biochem Cell Biol 1995;27:795–803.
Moberg F, Nystrom M, Kautsky N, Tedengren M, Jarayabhand P. Effects of reduced salinity on the rates of photosynthesis and respiration in the hermatypic corals *Porites lutea* and *Pocillopora damicornis*. Mar Ecol Prog Ser 1997;157:53–9.
Morrow G, Battistini S, Zhang P, Tanguay RM. Decreased lifespan in the absence of expression of the mitochondrial small heat shock protein Hsp22 in *Drosophila*. J Biol Chem 2004;279:43382–5.
Moyes CD, Moon TW, Ballantyne JS. Osmotic effects on amino acid oxidation in skate liver mitochondria. J Exp Biol 1986;125:181–95.
Muthiga NA, Szmant AM. The effects of salinity stress on the rates of aerobic respiration and photosynthesis in the hermatypic coral siderastrea siderea. Biol Bull 1987;173: 539–51.
Negishi M, Pedersen LG, Petrotchenko E, Shevtsov S, Gorokhov A, Kakuta Y, et al. Structure and function of sulfotransferases. Arch Biochem Biophys 2001;390:149–57.
Nicholson S. Ecocytological and toxicological responses to copper in *Perna veridis* hemocyte lysosomal membranes. Chemosphere 2001;45:399–407.
Orr AP, Moorehouse FW. Variations in physical and chemical conditions on and near Low Isles Reef. Scientific report of the great barrier reef expedition, vol. 2. London: British Museum (Natural History); 1933. p. 89–98.
Ornatsky OI, Connor MK, Hood DA. Expression of stress proteins and mitochondrial chaperonins in chronically stimulated skeletal muscle. Biochem J 1995;311:119–23.
Papp E, Nardai G, Soti C, Csermely P. Molecular chaperones, stress proteins and redox homeostasis. Biofactors 2003;17:249–57.
Pew Ocean Commission. 2003. America's living oceans: charting a course for sea change.
Porter JW, Lewis SK, Porter KG. The effect of multiple stressors on the Florida Keys coral reef ecosystem: a landscape hypothesis and a physiological test. Limnol Oceanogr 1999;44:941–9 1999.
Putnam NH, Srivastava M, Hellsten U, Dirks B, Chapman J, Salamov A, et al. Sea anemone genome reveals ancestral eumetazoan gene repertoire and genomic organization. Science 2007;6317:86–94.
Rankin JC, Davenport J. Animal osmoregulation. Glasgow: Blackie & Sons; 1981.
Reitzel AM, Sullivan JC, Traylor-Knowles N, Finnerty JR. Genomic survey of candidate stress-response genes in the estuarine anemone *Nematostella vectensis*. Biol Bull 2008;214:233–54.
Rensing SA, Goddemeier M, Hofmann CJ, Maier UG. The presence of a nucleomorph hsp70 gene is a common feature of Cryptophyta and Chlorarachniophyta. Curr Genet 1994;26:451–5.
Richmond RH. Effects of coastal runoff on coral reproduction. In: Ginsburg RN, editor. Proc Coll global aspects of coral reefs: health, hazards, and history. Miami: Rosenstiel School of Marine and Atmospheric Science; 1993. p. 360–4.
Rodriguez Milla MA, Maurer A, Rodriguez Huete A, Gustafson JP. Glutathione peroxidase genes in arabidopsis are ubiquitous and regulated by abiotic stresses through diverse signaling pathways. The Plant Cell 2003;36:602–15.
Ronis MJJ, Lindros KO, Ingelmann-Sundberg M. The CYP2E family. In: Ionnides C, editor. Cytochrome P450: metabolic and toxicological aspects. Boca Raton, FL: CRC Press; 1996. p. 211–39.
Sakaguchi S, Fukuda T, Takano H, Ono K, Takio S. Photosynthetic electron transport differentially regulates the expression of superoxide dismutase genes in liverwort, *Marchantia paleacea* var. *diptera*. Plant Cell Physiol 2004;45:318–24.
Schreiber U, Gademan R, Ralph PJ, Larkum AWD. Assessment of photosynthetic performance of Prochloron in *Lissoclonium patella* in hospite by chlorophyll fluorescence measurements. Plant Cell Physiol 1997;38:945–51.
Schwartsburd PM. Self-cytoprotection against stress: feedback regulation of heme-dependent metabolism. Cell Stress Chaperones 2001;6:1–5.
Scott JG, Wen Z. Cytochrome P450 of insects: the tip of the iceberg. Pesticide Management. Science 2001;57:958–67.
Shang F, Gong X, Taylor A. Activity of ubiquitin-dependent pathway in response to oxidative stress. J Biol Chem 1997;272:23086–93.
Shibahara S, Han F, Li B, Takeda K. Hypoxia and heme oxygenases: oxygen sensing and regulation of expression. Antioxid Redox Signal 2007;9:2209–25.

Shivakumar K, Jayaraman J. Salinity adaptation in fish: interaction of thyroxine with fish gill mitochondria. Arch Biochem Biophys 1986;245:356–62.
Snell TW, Brogdon SE, Morgan MB. Gene expression profiling in ecotoxicology. Ecotoxicology 2003;12:475–83.
Sokal RR, Rohlf FJ. Biometry. New York, New York: W.H. Freeman; 1995. p. 451–99.
Stocker R, Ames BN. Potential role of conjugated bilirubin and copper in the metabolism of lipid peroxides in bile. Proc Natl Acad Sci U S A 1987;84:8130–4.
Takahashi M, Hood MA. Protein import into subsarcolemmal and intermyofibrillar skeletal muscle mitochondria. Differential import regulation in distinct subcellular regions. J Biol Chem 1996;271:27285–91.
Thunell S, Harper P. Porphyrins, porphyrin metabolism, porphyries. III Diagnosis, care and monitoring in P*orphyria cutanea tarda* — suggestions for a handling programme. Scand J Clin Lab Invest 2000;60:561–80.
Tytlianov EA, Tsukahara J, Tytlianov TL, Leletkin VA, Van Woesik R, Yamazato K. Zooxanthellae population density and physiological state of the coral *Stylophora pistillata* during starvation and osmotic shock. Symbiosis 2000;28:303–22.
Van Woesik R, De Vantier LM, Glazebrook JS. Effects of cyclone "Joy" on nearshore corla communities of the Great Barrier Reef. Mar Ecol Prog Ser 1995;128:261–70.
Warner ME, Fitt WK, Schmidt GW. Damage to photosystem II in symbiotic dinoflagellates: a determinant of coral bleaching. Proc Natl Acad Sci USA 1999;96: 8007–12.
Willsie JK, Clegg JP. Small heat shock protein p26 associates with nuclear lamins and HSP70 in nuclei and nuclear matrix fractions from stressed cells. J Cell Biochem 2002;4:601–14.